doi:10.1093/brain/awl377 *Brain* (2007), **130**, 720–730

The topography of grey matter involvement in early and late onset Alzheimer's disease

Giovanni B. Frisoni,[1,2] Michela Pievani,[1] Cristina Testa,[1] Francesca Sabattoli,[1] Lorena Bresciani,[1] Matteo Bonetti,[3] Alberto Beltramello,[4] Kiralee M. Hayashi,[5] Arthur W. Toga[5] and Paul M. Thompson[5]

[1]Laboratory of Epidemiology Neuroimaging and Telemedicine, [2]Psychogeriatric Ward, IRCCS Centro San Giovanni di Dio FBF, The National Centre for Research and Care of Alzheimer's and Mental Diseases, [3]Service of Neuroradiology, Istituto Clinico Città di Brescia, Brescia, [4]Service of Neuroradiology, Ospedale Maggiore, Borgo Trento, Verona, Italy and [5]Laboratory of Neuroimaging, Department of Neurology, UCLA School of Medicine, Los Angeles, CA, USA

Correspondence to: Giovanni B. Frisoni, MD, Laboratory of Epidemiology, Neuroimaging and Telemedicine, IRCCS Centro San Giovanni di Dio FBF, The National Centre for Research and Care of Alzheimer's and Mental Diseases, via Pilastroni 4, 25125 Brescia, Italy
E-mail: papers@centroAlzheimer.it

Clinical observations have suggested that the neuropsychological profile of early and late onset forms of Alzheimer's disease (EOAD and LOAD) differ in that neocortical functions are more affected in the former and learning in the latter, suggesting that they might be different diseases. The aim of this study is to assess the brain structural basis of these observations, and test whether neocortical areas are more heavily affected in EOAD and medial temporal areas in LOAD. Fifteen patients with EOAD and 15 with LOAD (onset before and after age 65; Mini Mental State Examination 19.8, SD 4.0 and 20.7, SD 4.2) were assessed with a neuropsychological battery and high-resolution MRI together with 1:1 age- and sex-matched controls. Cortical atrophy was assessed with cortical pattern matching, and hippocampal atrophy with region-of-interest-based analysis. EOAD patients performed more poorly than LOAD on visuospatial, frontal-executive and learning tests. EOAD patients had the largest atrophy in the occipital [25% grey matter (GM) loss in the left and 24% in the right hemisphere] and parietal lobes (23% loss on both sides), while LOAD patients were remarkably atrophic in the hippocampus (21 and 22% loss). Hippocampal GM loss of EOAD (9 and 16% to the left and right) and occipital (12 and 14%) and parietal (13 and 12%) loss of LOAD patients were less marked. In EOAD, GM loss of 25% or more was mapped to large neocortical areas and affected all lobes, with relative sparing of primary sensory, motor, and visual cortex, and anterior cingulate and orbital cortex. In LOAD, GM loss was diffusely milder (below 15%); losses of 15–20% were confined to temporoparietal and retrosplenial cortex, and reached 25% in restricted areas of the medial temporal lobe and right superior temporal gyrus. These findings indicate that EOAD and LOAD differ in their typical topographic patterns of brain atrophy, suggesting different predisposing or aetiological factors.

Keywords: Alzheimer's disease; age at onset; magnetic resonance; hippocampus; computational neuroanatomy

Abbreviations: EOAD = early onset Alzheimer's disease; LOAD = late onset Alzheimer's disease; GM = grey matter; GMD = grey matter density

Received August 31, 2006. Revised October 26, 2006. Accepted December 15, 2006. Advance Access publication February 9, 2007

Introduction

Alois Alzheimer's first patient, Auguste D, whom he presented in Tubingen in 1906, was a 51-year-old woman with symptoms that would now be regarded as atypical for probable Alzheimer's disease (McKhann *et al.*, 1984). The symptoms included not only progressive cognitive impairment and psychosocial incompetence, but also focal symptoms and hallucinations (Maurer *et al.*, 1997). The belief that early and late onset Alzheimer's disease (EOAD and LOAD) may be different diseases persisted until 1984, when the currently accepted diagnostic criteria (McKhann *et al.*, 1984) collapsed the two entities under the unique rubric of Alzheimer's disease. This was based on the observation that the neuropathological hallmarks of EOAD and LOAD are the same (McKhann *et al.*, 1984). However, many research groups

have since continued to report phenotypic differences between EOAD and LOAD, with higher prevalence of language impairment or other neocortical functions (Maurer *et al.*, 1997; Klünemann *et al.*, 2002) and faster cognitive deterioration (Rogaeva, 2002), more severe perfusion and metabolic deficits in the temporal and parietal areas (Lantos *et al.*, 1992; Mann *et al.*, 1996; Fukutani *et al.*, 1997), and greater grey matter (GM) atrophy (Chui *et al.*, 1985) in EOAD. Recent studies showing that EOAD but not LOAD may be lacking in adult neurogenesis (Wang *et al.*, 2004; Boekhoorn *et al.*, 2006), a phenomenon believed to be a compensatory attempt to counterbalance the active process of neuronal loss, has revived interest in the topic and supported the notion that the causal mechanisms underlying the two forms of the disease may be at least partly different.

To date, few studies have compared the amount and location of brain tissue loss in EOAD and LOAD. In a previous study, we compared high resolution structural MR images of nine EOAD and nine severity-matched LOAD patients to 26 age-matched controls (Frisoni *et al.*, 2005). With the use of voxel-based morphometry, we found greater temporoparietal GM atrophy in EOAD and greater medial temporal atrophy in LOAD, in agreement with previous imaging studies and neuropsychological work suggesting greater memory impairment in LOAD and impairment of neocortical functions in EOAD (Seltzer and Sherwin, 1983; Chui *et al.*, 1985; Grady *et al.*, 1987; Jacobs *et al.*, 1994; Sakamoto *et al.*, 2002; Kemp *et al.*, 2003). However, the study had some limitations in that the algorithms we used allow to map atrophy only approximately (with a precision of 5–10 mm), only the significance of the difference was assessed, and no information was provided regarding neuropsychological test performance and the proportion of tissue lost.

We therefore aimed, in the present study, to quantify and map cortical GM and hippocampal atrophy in a sizable group of well-studied EOAD and LOAD patients, contrasting the 3-dimensional patterns of atrophy.

Material and methods

Participants and assessment

Patients were selected from a group of 68 enrolled in a project to detect *in vivo* structural brain changes in the neurodegenerative dementias using advanced neuroimaging techniques at the IRCCS Centro San Giovanni di Dio Fatebenefratelli (National Center for Alzheimer's Disease), in Brescia, Italy, between November 2002 and August 2005.

Each patient underwent: (i) history taking, (ii) laboratory exams, (iii) physical and neurological examination, (iv) neuropsychological assessment, and (v) MRI scanning. History was taken with a structured interview from patients' relatives (usually spouses) and age at onset was estimated from the caregiver's report of memory disturbances exceeding the episodic forgetfulness that might be regarded as usual for the patient or report of other progressive disturbances (language, praxis, orientation, visuospatial skills) (Frisoni *et al.*, 1996). Laboratory exams included complete blood count, chemistry profile, thyroid function, B12 and folic acid and EKG. Physical examination was performed by a geriatrician and neurological examination by a neurologist. Neuropsychological assessment was performed by a psychologist and assessed: (i) global cognitive functioning with the Mini Mental State Examination (Folstein *et al.*, 1975), (ii) language with letter and category fluency (Novelli *et al.*, 1986) and token tests (De Renzi and Vignolo, 1962; Spinnler and Tognoni, 1987), (iii) visuospatial functions with the Rey figure copy test (Caffarra *et al.*, 2002), (iv) frontal-executive functions with the Trail Making Test (Reitan, 1958; Amodio *et al.*, 2002), and (v) learning with Rey's word list immediate and delayed recall (Carlesimo *et al.*, 1996) and Rey figure delayed recall (Caffarra *et al.*, 2002) tests. The diagnosis of probable Alzheimer's disease was made according to common research criteria (McKhann *et al.*, 1984). Genomic DNA was extracted from whole-blood samples of subjects according to standard procedures. *APOE* genotyping was carried out by PCR amplification and *Hha*I restriction enzyme digestion. The genotype was resolved on 4% Metaphor Gel (BioSpa, Italy) and visualized by ethidium bromide staining (Hixson and Vernier, 1990).

Of the original group of 68 Alzheimer's disease patients, 17 were 65 years old or younger at disease onset (EOAD). None had family history suggestive of autosomal dominant disease. Two of the EOAD patients were excluded from the analysis due to MRI artefacts leaving 15 for analysis. Fifteen patients were then selected from those 51 with onset after age 65 (LOAD) in order to match EOAD patients by dementia severity as measured by the Clinical Dementia Rating (Hughes *et al.*, 1982). When more than one matching LOAD patient was available, the one with the closest matching Mini Mental State Examination was chosen. The group size of 15 for LOAD was chosen to preserve similar power for the EOAD and LOAD analyses.

Thirty age- and sex-matched healthy subjects were selected from those enrolled in a study on normal brain structure with MRI (ArchNor, Normative Archive of Structural Brain Magnetic Resonance Imaging), as described in detail elsewhere (Riello *et al.*, 2005). Healthy subjects were matched 1:1 to the EOAD and LOAD groups based on age and sex, and underwent multidimensional assessment including clinical, neurological and neuropsychological evaluations.

Written informed consent was obtained from patients and controls. No compensation was provided for study participation. The study was approved by the local ethics committee.

MR imaging

MRI scans were acquired with a Philips Gyroscan 1.0 T at the Neuroradiology Unit of the Città di Brescia hospital in Brescia. High-resolution gradient echo sagittal 3D sequences (TR = 20 ms, TE = 5 ms, flip angle = 30°, field of view = 220 mm, acquisition matrix = 256 × 256 and slice thickness = 1.3 mm) were used for cortical pattern matching and hippocampal and lobar volume measurements, axial dual echo (TR = 2000 ms, TE = 8.8/110 ms, flip angle = 90°, field of view = 230 mm, acquisition matrix = 256 × 256, slice thickness = 5 mm) and FLAIR sequences (TR = 5000 ms, TE = 100 ms, flip angle = 90°, field of view = 230 mm, acquisition matrix = 256 × 256, slice thickness = 5 mm) were used to assess subcortical cerebrovascular

disease with the age-related white matter changes (Wahlund *et al.*, 2001) scale (total score ranging between 0 and 30).

Global (volumetry) and local (mapping) analyses were carried out on the GM and hippocampus. Cortical GM was studied with the cortical pattern matching algorithms developed at the Laboratory of Neuroimaging (LONI) of the University of California at Los Angeles (Thompson *et al.*, 2004). The hippocampus was studied with region-of-interest analyses.

Grey matter

Cortical mapping. The 3D images were reoriented along the AC-PC line and voxels below the cerebellum were removed with the MRIcro software (www.psychology.nottingham.ac.uk/staff/cr1/mricro.html). The anterior commissure was manually set as the origin of the spatial coordinates for an anatomical normalization algorithm implemented as part of Statistical Parametric Mapping (SPM99) software package (www.fil.ion.ucl.ac.uk/spm). A 12-parameter affine transformation was used to normalize each image to a customized template in stereotaxic space, created from the MRI scans of 40 control subjects.

Individual brain masks for each hemisphere were extracted from normalized images with the automatic method EMS (expectation maximization segmentation; www.medicalimagecomputing.com/EMS) (Van Leemput *et al.*, 1999*a*; Van Leemput *et al.*, 1999*b*), visually inspected, and manually corrected with DISPLAY, a three-dimensional visualization program that enables simultaneous viewing of sagittal, coronal and axial slices of the brain (http://www.bic.mni.mcgill.ca/software/Display/Display.html), and allows the manual correction of errors between brain and non-brain tissue. The resulting masks were then applied to normalized images to obtain 'skull-stripped' images of each hemisphere. A 3D model of hemispherical cortical surfaces was automatically extracted using intensity information (MacDonald *et al.*, 1994). Normalized images were segmented into GM, white matter and cerebrospinal fluid using an algorithm that employs partial volume correction and bias field correction (Shattuck *et al.*, 2001).

Sulcal lines were traced by a single tracer (M.P.) on the cortical surfaces according to a previously validated anatomical delineation protocol (http://www.loni.ucla.edu/~khayashi/Public/medial_surface, http://www.loni.ucla.edu/~esowell/new_sulcvar.html). For each subject 17 sulci were manually outlined on the lateral surface of each hemisphere, and a set of 12 sulci were traced on the medial surface; additional 3D lines were drawn to outline interhemispheric gyral limits. The reliability of manual outlining was assessed prior to experimental subject tracing with a standard protocol requiring the same rater to trace all lateral and medial sulci of six test brains (Sowell *et al.*, 2002). At the end of the reliability phase, the mean 3D difference of the tracer from the gold standard was <3 mm everywhere for the medial sulci and <4.5 mm everywhere for the lateral sulci.

Sulcal curves and cortical surfaces were flattened and averaged across subjects to create a population specific template based on all the subjects in the study (Thompson *et al.*, 2000). Averaged sulci were then used as landmarks to warp each subject's anatomy into the template. The same deformation was applied to the segmented images, thus allowing measurement of GM at thousands of homologous cortical locations. Grey matter density (GMD) was computed at each cortical point as the proportion of GM tissue classified as GM in a sphere centred at that point, with a radius of 15 mm, and then averaged within each group to obtain the GMD mean.

Lobar volumetry. One scan from a young and one from an older control subject representative of the average atrophy of control groups, served as reference atlases for the appropriate patients and control groups. The atlases were manually edited to outline regions of interest comprising frontal, temporal, parietal, and occipital lobes (http://www.loni.ucla.edu/NCRR/Protocols/MaskingRegions.shtml). Since cortical surfaces were elastically matched during cortical pattern matching, this elastic deformation was used to map the reference labels to each individual's surface of the corresponding group. The individual labels obtained in this way were applied to the corresponding GMD image and volumes at each cortical point were averaged and compared across groups by pooling GMD values over homologous cortical lobar locations defined by the manually defined cortical sulci.

A map of the average percentage GM reduction was computed based on the ratio, at each cortical point, between the mean GMD value at that point in each Alzheimer's disease patient group (EOAD and LOAD) and the GMD mean of the pertinent control group. This ratio allows a map of the relative deficit in GM to be visualized, as a proportion, or percentage of the normal values seen in healthy controls.

Hippocampus

Volumetry. The 3D images were processed using a combination of scripts written in Perl (http://www.perl.com) based on software developed at the McConnel Brain Imaging Centre (Montreal Neurological Institute, McGill University, Montreal, Canada). Processing includes correction for magnetic field non-uniformities, intensity normalization and brain-to-brain linear registration to a standard template in the stereotaxic space (ICBM152) based on the Talairach atlas (Collins *et al.*, 1994). Each registered image was visually compared with the ICBM152 template using the software program REGISTER (McGill University, Montreal, Canada) and, when the automatic registration failed (mainly due to high scalp brightness), a manual registration was performed, based on eleven anatomical landmark points, distributed over the cerebrum and brainstem (the most anterior point of the temporal poles, the most posterior aspect on the occipital lobe, the most anterior point on the frontal lobe, the central sulcus, the inferior ventral aspect of the pons–midbrain cleft, the genu and splenium of the corpus callosum, the interthalamus adhesion and the eyes). The hippocampi were manually traced by an expert tracer (L.B.) with the software program DISPLAY (McGill University, Montreal, Canada) on contiguous coronal 1.5 mm thick images, simultaneously checking tracing accuracy on the sagittal and axial planes. Test–retest reliability on 20 patients and controls was good – intraclass correlation coefficients were 0.96 for the right and 0.94 for the left hippocampus. The anatomical starting point was the hippocampal head when it first appears below the amygdala, the alveus defining the superior and anterior border of the hippocampus. The fimbria was included in the hippocampal body, while the GM rostral to the fimbria was excluded. The hippocampal tail was traced until it was visible as an oval shape located caudally and medially to the trigone of the lateral ventricles (Pruessner *et al.*, 2000). To obtain the original hippocampal volume (i.e., in the native scanner space), the brain with the traced region of interest was back-transformed from the stereotaxic to the native space.

The total intracranial volume (TIV) was obtained by manually tracing with the software DISPLAY the entire intracranial cavity (the lower boundary being the foramen magnum) on 7 mm thick

Table 1 Sociodemographic and clinical features of 15 early onset (EOAD), 15 late onset (LOAD) Alzheimer's disease patients matched to EOAD based on clinical dementia rating, and 1:1 age-and sex-matched controls

	EOAD		LOAD	
	Patients	Controls	Patients	Controls
Age, years	62.5 (4.7)	62.5 (5.4)	78.5 (6.2)	76.8 (3.4)
Sex, females	10 (67%)	10 (67%)	12 (80%)	12 (80%)
Education, years	7.7 (5.6)	9.1 (4.1)	4.6 (1.2)	8.7 (4.2)
Clinical dementia rating, 0.5/1/2	3/11/1	–	3/11/1	–
Mini Mental State Examination	19.8 (4.0)	28.7 (0.9)	20.7 (4.2)	28.0 (1.3)
Disease duration, years	3.1 (1.7)	–	3.3 (1.6)	–
Age at onset, years	59.5 (4.5)	–	75.1 (6.9)	–
ApoE e4 allele	7 (47%)	4 (27%)	7 (47%)	2 (13%)
White matter disease	1.7 (2.1)	2.6 (4.9)	5.4 (5.0)	2.5 (2.2)

Values denote mean (standard deviation) or number (percentage). White matter disease was assessed with the Age-Related White Matter Changes scale, ranging from 0 to 30 (Wahlund *et al*., 2001).

coronal slices. Native hippocampal volumes were normalized to the TIV by dividing individual hippocampal volumes by the individual TIV and multiplying by the TIV grand mean. TIV was 1384 (SD 151) versus 1481 cc (SD 146, $P = 0.059$) in EOAD *versus* corresponding young controls and 1340 (SD 123) versus 1433 cc (SD 96, $P = 0.021$) in LOAD *versus* corresponding older controls.

Percentage hippocampal reduction was computed as the ratio between the hippocampal volume of each individual Alzheimer's disease patient and the mean of the pertinent control group.

Statistical analysis

Clinical, sociodemographic, neuropsychological, hippocampal and lobar volumetric data were analysed using Student's *t*-test for continuous variables and the χ^2 test for dichotomous variables. Significant results of the *t*-test were confirmed with a non–parametric test (Mann–Whitney U-test).

The effect of diagnosis (Alzheimer's disease versus controls) and age ($\leqslant 65$ versus >65), and their interaction on neuropsychological tests, lobar and hippocampal volumes was assessed with analysis of variance (ANOVA). The significance of the interaction was tested in a full factorial model, i.e. including the two main effects of diagnosis and age, and their interaction. As both Alzheimer's disease groups had test scores poorer and brain volumes lower than the pertinent control group, significance of the interaction denoted a relatively poorer performance or relatively lower volumes in one of the two patient groups.

Cortical pattern matching analyses were carried out assessing the correlation between GMD and diagnosis (assigning value '0' to controls and '1' to Alzheimer's disease subjects) to identify cortical GM loss in (i) EOAD and (ii) LOAD compared with their pertinent control group. The resulting significance and percentage reduction maps showed the topographic distribution of the effect of diagnosis on GMD in the whole cortex, and were corrected for multiple comparisons running permutation test at a threshold of $P = 0.01$. This test produces a corrected overall *P*-value for the uncorrected statistical maps, computing the chance of the observed pattern occurring by accident (Thompson *et al*., 2003).

Results

Clinical and neuropsychological features

Table 1 shows that the EOAD and LOAD groups were appropriately matched to the pertinent control groups for age and sex ($P > 0.36$ on *t*-test and χ^2 test). The age range was 53.9–69.2 years in EOAD, 52.0–68.9 in young controls, 71.0–89.6 in LOAD, and 72.2–84.2 in older controls. Education was about 3 years higher on average in EOAD than LOAD ($P = 0.051$ on *t*-test). Due to this matching, EOAD and LOAD groups had the same clinical dementia rating distribution, and also Mini Mental State Examination and disease duration were similar ($P > 0.55$). The first symptoms of the disease had started around age 60 in the EOAD and 15 years later in the LOAD patients. EOAD and LOAD groups had the same frequency of the *APOE* e4 allele; the frequency was proportionally higher than in controls for both LOAD and EOAD, but not significantly ($P > 0.25$ on χ^2 test). White matter disease showed a trend for being higher in patients than controls in LOAD ($P = 0.055$ on *t*-test); the difference between EOAD patients and controls was not significant ($P = 0.53$). Control groups were not different on white matter disease ($P = 0.96$), while LOAD had more severe white matter disease than EOAD ($P = 0.017$).

Table 2 shows that patients performed significantly more poorly than control subjects on almost all neuropsychological tests—except in the case of the LOAD group on the token and trail making B-A tests. Performance was relatively poorer in EOAD than LOAD (interaction term significant on ANOVA) for visuospatial, frontal-executive and learning tests. The individual neuropsychological profile of EOAD and LOAD patients are given in the supplementary Table S1 and Table S2.

Volumetry

Volumetric analysis showed significant GM atrophy (both lobar and hippocampal) in EOAD and LOAD relative to

Table 2 Neuropsychological features of EOAD and LOAD patients and controls

		EOAD			LOAD			
		Patients	Controls	*P*	Patients	Controls	*P*	*P* of interaction on ANOVA
Language	Letter fluency	25 (9)	37 (11)	0.007	25 (9)	35 (8)	0.010	0.834
	Category fluency	24 (10)	42 (8)	<0.001	26 (5)	40 (6)	<0.001	0.331
	Token test	26.1 (8.3)	32.7 (1.3)	0.009	27.9 (4.9)	31.0 (4.1)	0.125	0.258
Visuospatial	Rey figure copy	7 (11)	36 (1)	<0.001	17 (10)	36 (2)	<0.001	0.032
Frontal-executive	Trail Making Test A	226 (111)	24 (13)	<0.001	130 (70)	25 (14)	<0.001	0.018
	Trail Making Test B	388 (122)	45 (36)	<0.001	216 (64)	63 (52)	<0.001	<0.001
	Trail Making Test B-A	162 (83)	21 (29)	<0.001	82 (71)	39 (48)	0.122	0.008
Learning	Rey list immediate recall	18 (7)	48 (7)	<0.001	28 (6)	48 (8)	<0.001	0.026
	Rey list delayed recall	2.1 (1.9)	11.6 (2.6)	<0.001	3.6 (1.1)	10.9 (2.4)	<0.001	0.062
	Rey figure recall	4 (4)	21 (6)	<0.001	10 (3)	20 (6)	0.001	0.008

Values denote mean (standard deviation). *P* denotes significance on *t*-test. *P* of interaction on ANOVA denotes significance of the age × diagnosis interaction term. Test scores are age- sex- and education-adjusted. Alzheimer's patients have poorer performance than matched controls in almost all tests. For visuospatial, frontal-executive, and learning tests the performance of EOAD is relatively poorer than that of LOAD patients (significant *P* of the interaction term on ANOVA).

Table 3 Lobar cortical GM and hippocampal volumetric features of EOAD and LOAD patients and controls

		EOAD			LOAD			
		Patients	Controls	*P*	Patients	Controls	*P*	*P* of interaction on ANOVA
Frontal	L	69.6 (6.6)	82.6 (6.3)	<0.001	62.1 (7.6)	68.5 (5.4)	0.013	0.053
	R	66.2 (6.5)	82.1 (7.7)	<0.001	64.3 (7.7)	71.9 (5.1)	0.004	0.021
Temporal	L	38.3 (3.4)	46.5 (3.7)	<0.001	39.2 (3.9)	45.5 (4.1)	<0.001	0.320
	R	40.5 (4.7)	51.8 (5.7)	<0.001	38.1 (4.5)	45.3 (3.4)	<0.001	0.101
Parietal	L	22.5 (1.9)	29.0 (2.7)	<0.001	21.9 (2.0)	25.2 (1.2)	<0.001	0.003
	R	21.1 (2.3)	27.2 (3.4)	<0.001	21.2 (2.3)	24.0 (1.5)	0.001	0.012
Occipital	L	10.3 (1.0)	13.7 (1.4)	<0.001	9.3 (0.7)	10.6 (1.0)	<0.001	<0.001
	R	11.6 (1.3)	15.0 (1.7)	<0.001	10.2 (1.1)	11.8 (0.9)	<0.001	0.011
Total grey matter	L	140.6 (11.3)	171.9 (12.8)	<0.001	132.6 (13.4)	149.8 (10.7)	0.001	0.027
	R	139.3 (13.4)	176.0 (17.3)	<0.001	133.8 (14.7)	153.0 (9.7)	<0.001	0.019
Hippocampus	L	2458 (252)	2726 (277)	0.010	2151 (391)	2701 (324)	<0.001	0.088
	R	2469 (323)	2945 (358)	0.001	2215 (499)	2827 (589)	0.005	0.564

L = left, R = right. Lobar volumes are expressed in cm^3, hippocampal volumes in mm^3. Values denote mean (standard deviation). *P* denotes significance on *t*-test. *P* of interaction on ANOVA denotes significance of the age x diagnosis interaction term. A significant interaction denotes that the grey matter loss of EOAD patients relative to younger controls is disproportionally greater than that of LOAD patients relative to older controls. In the frontal, parietal and occipital lobes and total grey matter, volumes were relatively smaller in EOAD than LOAD patients (significant *P* of the interaction term on ANOVA), indicating relatively greater atrophy in EOAD. In the left hippocampus a trend to significance speaks for the opposite effect, i.e. relatively greater atrophy in LOAD.

their matched controls (Table 3). Total GM atrophy was greater in EOAD than LOAD (left: $P = 0.027$ for the interaction term on ANOVA; right: $P = 0.019$), and lobar analyses allowed us to localize this effect to the occipital (left: $P < 0.001$; right: $P = 0.011$), parietal (left: $P = 0.003$; right: $P = 0.012$), and right frontal lobe (left: $P = 0.053$; right: $P = 0.021$), while atrophy in the temporal lobes was similar in the two patient groups ($P > 0.100$). In the left hippocampus a trend for significance ($P = 0.088$) provided some evidence for the opposite effect, i.e., relatively greater atrophy in LOAD.

Total GM loss was 19.5% in EOAD and about half as large (11.9%) in LOAD when compared with matched controls (data not shown). The largest GM percentage reduction for EOAD patients was in the occipital lobe (23.8% average loss between right and left side) and for LOAD patients the largest GM percentage reduction was in the hippocampus (21.1% loss, Fig. 1). Hippocampal volume reduction in EOAD (13.1%) and occipital GM reductions in LOAD patients (12.3%) were less marked. The comparison of percentage reductions between EOAD and LOAD achieved statistical significance in the occipital lobes (left: $P < 0.001$ on *t*-test, right: $P = 0.012$), parietal (left: $P = 0.001$, right: $P = 0.002$), and right frontal lobe ($P = 0.016$) with a trend to significance in the left ($P = 0.077$), and total GM (left: $P = 0.026$, right: $P = 0.014$),

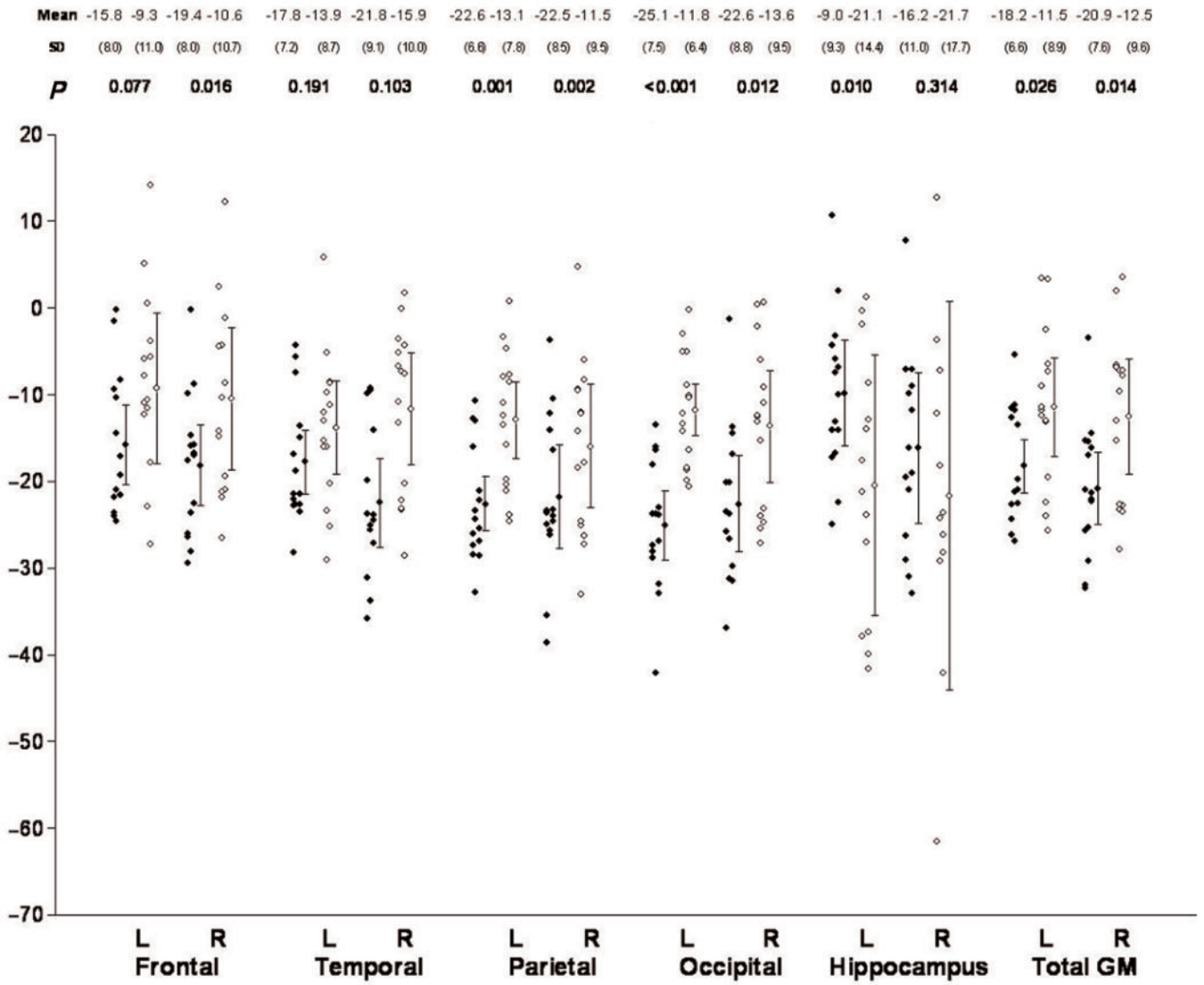

Fig. 1 Lobar and hippocampal GM atrophy of EOAD compared with LOAD patients. The figure shows individual data points of percentage reduction, error bars denote mean and 95% confidence intervals, and the table above reports mean values, standard deviations (SD), and *P* on *t*-test. EOAD showed greater grey matter reduction than LOAD in all lobes, with significant difference in the parietal, occipital, right frontal and a trend to significance in the left frontal lobes. Conversely, LOAD showed a greater hippocampal reduction than EOAD on the left side. GM = grey matter; L = left; R = right; ◆ Early onset and ◇ late onset Alzheimer's disease.

while the difference was not significant in temporal lobes (left: $P = 0.191$, right: $P = 0.103$). In the left but not the right hippocampus a statistical difference was present indicating greater atrophy in LOAD (left: $P = 0.010$, right: $P = 0.314$). Significance values were confirmed with Mann–Whitney U-test for all comparisons except in the left frontal lobe, where the trend toward significance on *t*-test disappeared altogether ($P = 0.110$). The different pattern of atrophy in the parietal, occipital, and frontal lobes and hippocampus in EOAD and LOAD was tested in an ANOVA model where age ($\leqslant 65$ versus >65) was a between-subject factor, site (frontal versus hippocampus, parietal versus hippocampus and occipital versus hippocampus) were within-subject factors, and percentage reduction was treated as the dependent variable. This confirmed that the patterns of frontal-parietal-occipital and hippocampal atrophy were different in EOAD and LOAD (left: $F(1,28) > 9.1$, $P < 0.005$; right: $F(1,28) > 4.8$, $P < 0.038$).

Cortical mapping

Cortical pattern matching analysis showed that in EOAD statistically significant GM reduction was widespread (Fig. 2, left), involving the frontal, temporal, parietal and occipital cortex including the posterior cingulate and the retrosplenial region, and sparing only the somatosensory and primary visual cortex, the anterior cingulate gyrus and the orbitomesial cortex (permutation test: $P = 0.0001$ for both the left and right hemispheres). Conversely, in LOAD patients statistically significant GM reduction was located in

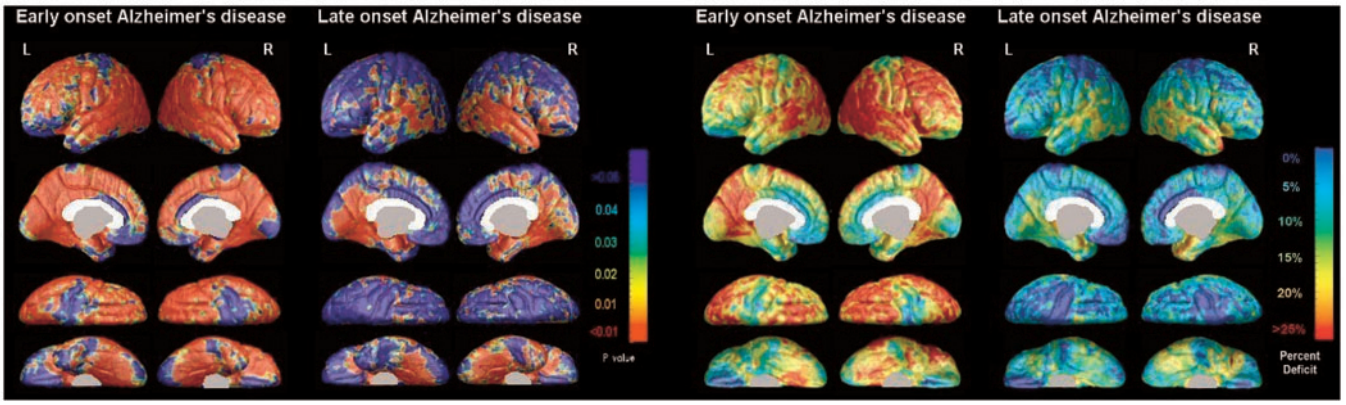

Fig. 2 Grey matter loss of EOAD and LOAD patients compared with controls. *Left*: significance map, the colour bar denoting significance of GM loss between patients and controls (regions in red correspond to $P < 0.01$). EOAD had significant atrophy of most of the neocortex, sparing only part of the primary sensory, motor, and visual cortex, anterior cingulate and orbital cortex. Atrophy in LOAD patients was confined to the medial temporal and retrosplenial areas, superior and middle temporal gyri, and temporoparietal junction. *Right*: percentage reduction map, the colour bar denoting the proportion of GM loss in patients versus controls (regions in red correspond to loss of 25% or greater). In EOAD, GM loss is of 25% or higher in large neocortical areas. The EOAD maps allow to more clearly appreciate the relative sparing of the primary sensory, motor, and visual cortex, anterior cingulate and orbital cortex as well as the right greater than left involvement. In LOAD, GM loss is markedly milder, being between 15 and 20% in the temporoparietal and retrosplenial cortex, and reaching 25% in restricted areas of the medial temporal lobe and right superior temporal gyrus.

the temporal, retrosplenial cortex, and the temporoparietal junction (permutation test: $P = 0.0027$ in the left and $P = 0.0019$ in the right hemisphere; Fig. 2, left). The significance pattern was replicated in the percentage reduction maps: in EOAD, GM loss of 25% or more (Fig. 2, right) mapped to large neocortical areas affecting all lobes, with relative sparing of the left frontal and anterior temporal lobes, and preservation of primary sensory, motor, and visual cortex, and anterior cingulate and orbital cortex. In LOAD, GM loss was diffusely milder (below 15%), with losses between 15 and 20% confined to part of the temporoparietal and retrosplenial cortex. Losses reached 25% in restricted areas of the medial temporal lobe and right superior temporal gyrus. The different degree of GM loss in EOAD and LOAD was confirmed with multiple regression analysis, entering age and diagnosis as covariates and mapping the interaction term (Supplementary Fig. S1).

Discussion

In this study we have shown that EOAD patients, on average, have more severe GM atrophy than LOAD patients matched for dementia severity, and that atrophy has a topographic specificity, being more severe in neocortical areas in EOAD, and in the hippocampus in LOAD.

Disease aggressiveness of EOAD and LOAD

The greater GM atrophy in EOAD than LOAD patients of similar clinical severity raises the possibility that EOAD is a more aggressive form of disease. However, this is not necessarily the case as GM volume at the time of diagnosis is not only a function of disease aggressiveness (i.e. the level of plaque and tangle deposition) but also of cognitive reserve (i.e. the synaptic or neuronal redundancy that makes the brain more or less susceptible to developing symptoms with a given degree of plaque and tangle load) and of age at biological onset (i.e. the time when plaque and tangle deposition starts). It is now widely accepted that the pathological hallmarks of Alzheimer's disease (amyloid plaques and neurofibrillary tangles) appear in the brain starting decades before the first appearance of symptoms and accumulate steadily involving progressively more widespread cortical areas (Braak *et al.*, 1998; Smith, 2002). In the patients of this study, we have no reason to believe that cognitive reserve was, or is generally, different between EOAD and LOAD patients.

Cognitive reserve is known to be associated with educational level (persons with greater education have greater brain reserve) and *APOE* genotype (carriers of the e4 allele have lower brain reserve). Our EOAD patients had 3 years more schooling than LOAD on average, which should denote greater functional reserve and delay clinical onset in EOAD. The e4 allele of *APOE* was equally prevalent in EOAD and LOAD. Whatever a patient's age is at biological onset (and no information is available on this), the only possible scenario that is consistent with biological disease severity being greater and age at onset younger in EOAD—and cognitive reserve being equal in the two groups—is one where the aggressiveness of the disease is greater in EOAD. It needs to be stressed that this scenario assumes that brain atrophy is proportional to biological disease severity (i.e. plaque and tangle load), that age-associated atrophy is minor or negligible compared with that associated with disease, and Alzheimer's-associated

atrophy is either linear over time or has the same time course in EOAD and LOAD. While the first two assumptions seem to find support in the literature (DeCarli *et al.*, 1994; Gosche *et al.*, 2002), the latter is more disputable as a recent observation has shown that atrophy accelerates during the course of the disease in EOAD (Chan *et al.*, 2003). However, whether this time course is similar in LOAD is presently unknown. The finding of greater aggressiveness of the disease in EOAD is in agreement with observations of faster clinical progression and ventricular dilatation (Jacobs *et al.*, 1994; Kono *et al.*, 1994; Ho *et al.*, 2002), faster deposition of pathology in early-onset familial Alzheimer's disease brains (Gomez-Isla *et al.*, 1999), and absence of adult neurogenesis in EOAD but not LOAD (Jin *et al.*, 2004; Boekhoorn *et al.*, 2006). In other neuropsychiatric diseases, e.g. schizophrenia, the earlier onset form is also typically associated with poorer outcomes and refractoriness to treatment (Sheitman and Lieberman, 1998).

The posterior limbic system in EOAD and LOAD

The results of this study support the widely held belief that Alzheimer's disease affects the posterior sector of the limbic system as defined by the connectivity of the cingulate cortex, and confirms that this is the case in both EOAD and LOAD. The posterior limbic system is comprised of the posterior cingulate gyrus and its most strictly interconnected structures, i.e. the temporoparietal, retrosplenial and entorhinal cortex and the hippocampus. It is thought to integrate the evaluative aspects of information from the environment and the organism itself (Vogt *et al.*, 1992). Interestingly, the ventromedial prefrontal and anterior cingulate cortex, belonging to the anterior sector of the limbic system based on their cingulate connectivity, are selectively spared in both EOAD and LOAD. The ventromedial prefrontal and anterior cingulate cortex is the largest cortical area of the rostral limbic system, believed to integrate aspects related to the execution of behavioural output (Vogt *et al.*, 1992; Devinsky *et al.*, 1995). We recently proposed that the rostral limbic system is specifically affected by a form of neurodegenerative dementia separate from Alzheimer's disease, i.e. frontotemporal lobar degeneration (Boccardi *et al.*, 2005). As frontotemporal lobar degeneration is caused by intracellular deposition of abnormally phosphorylated tau protein (de Silva *et al.*, 2006), it is tempting to speculate on the network specificity of the two pathogenic proteins, with amyloid affecting the posterior and tau affecting the rostral limbic system structures.

Indeed, amyloid deposition, starting from medial temporal regions (Smith, 2002) affects the posterior limbic system due to its close connections to the posterior sector of the cingulate gyrus (Vogt *et al.*, 1992). Indeed, hypometabolism of the posterior cingulate is observed very early in Alzheimer's disease progression, when no atrophy can yet be detected in this region (Mosconi *et al.*, 2004; Hirao *et al.*, 2006). On the other hand, in frontotemporal lobar degeneration, neuronal loss is first observed in the frontal regions closely connected to the anterior cingulate cortex (Kril and Halliday, 2004). The reason why amyloid deposits first in the medial temporal regions while tau in the frontal cortex is still unknown, and might depend on structural, functional, or molecular vulnerability to pathogenic proteins.

Natural history and predisposing factors of EOAD and LOAD

Within the posterior limbic system, the topographic specificity of EOAD affecting mainly the parietal associative cortex, and LOAD the hippocampus is in agreement with previous observations on atrophic changes with magnetic resonance (Frisoni *et al.*, 2005; Shiino *et al.*, 2006) and on blood perfusion with single photon emission tomography (Kemp *et al.*, 2003). This indicates that EOAD and LOAD may arise with differing natural history and topography of disease neurobiology and, perhaps, also with different predisposing factors.

Neurochemical and neuroimaging studies support the view that plaques and tangles might deposit earlier or more heavily in the neocortex and later or less heavily in the hippocampal regions in EOAD, and the opposite might occur in LOAD. Choline acetyl-transferase has been found to be significantly lower in EOAD than in controls in extensive brain areas including the frontal and temporal cortex, while choline acetyl-transferase activity in LOAD was significantly lower than in age-matched controls only in the hippocampus (Bird *et al.*, 1983). Another study assessing choline acetyl-transferase as well as γ-aminobutyric acid (GABA) and somatostatin found widespread reductions in the concentration of all neurotransmitters in EOAD, while in LOAD the deficit was confined to the cholinergic enzyme in the temporal lobe and hippocampus (Rossor *et al.*, 1984). More recent studies of familial Alzheimer's disease in subjects with known presenilin mutations have found extensive Aβ deposits in the frontal, temporal, parietal, and occipital neocortex, but fail to explicitly address the medial temporal lobe (Haltia *et al.*, 1994; Singleton *et al.*, 2000; Larner and du Plessis, 2003). Prospective structural studies with high resolution MR imaging in familial EOAD have shown significant volumetric reductions in both the medial temporal lobe and parietal association cortex, but an estimate of the magnitude of the change has not been provided (Fox *et al.*, 2001; Scahill *et al.*, 2002). A study on four brains with a PS1 mutation showed the greatest A-beta$_{40}$ amyloid burden in the occipital lobe (Lemere *et al.*, 1996). Visual inspection of the voxel compression maps denoting progression of cortical atrophy in an asymptomatic 36-year-old woman

with familial Alzheimer's disease suggested that subarachnoid and ventricular space dilation over 4 years was greater in proximity to the parietal than the medial temporal region (Fox *et al.*, 2001).

The known greater relative effect of heredity on neocortical structure and greater environmental effects on medial temporal structures (Sullivan *et al.*, 2001; Thompson *et al.*, 2001) speaks for greater genetic predisposition in EOAD and environmental exposures in LOAD. Genes play a relevant role in EOAD (Janssen *et al.*, 2003) and yet unknown genetic factors might confer on neocortical regions a greater susceptibility to Alzheimer's disease. This hypothesis is consistent with the twin studies of Thompson and colleagues, who showed that frontal, linguistic and parietooccipital areas (including the temporoparietal cortex) are under strict genetic control, with 95–100% of the variance being attributable to genetic factors (Thompson *et al.*, 2001). On the contrary, the hippocampus is controlled by genes to a lesser degree, these explaining only about 40% of the variance of hippocampal volumes (Sullivan *et al.*, 2001). These observations suggest that genetic factors may drive the susceptibility to developing Alzheimer's disease lesions in the neocortex in young age, while environmental factors might exert a similar effect on medial temporal lobe structures at older age.

An incidental finding of the present study confirms previous speculations of smaller brain size as a possible risk factor for Alzheimer's disease (Mori *et al.*, 1997). Indeed, in both EOAD and LOAD, the total intracranial volume was about 7% smaller than that of correspondent age-matched controls.

Topographic correspondence of neuropsychological deficits

The dissociation between neocortical and hippocampal atrophy in EOAD and LOAD is only partly in agreement with neuropsychological tests. In fact, while visuospatial and frontal-executive tests were disproportionately poorer in EOAD than LOAD, in agreement with the greater neocortical atrophy of EOAD, learning tests were not poorer in LOAD as the greater hippocampal involvement would lead one to expect. A possible explanation might lie in the fact that the learning tests we used are dependent on neocortical functions such as language and constructional praxis, which might attenuate the effect of relatively preserved learning in EOAD. The use of language- and praxis-independent tests specific to episodic memory might provide a better estimate of patients' memory abilities.

Methodological issues

The present findings expand on those of a previous SPM-based voxel-based morphometry study on an independent group of nine EOAD and nine LOAD patients compared with 26 controls where we found greater temporoparietal atrophy in EOAD and greater medial temporal atrophy in LOAD (Frisoni *et al.*, 2005). None of the subjects of the former study is included in the present study and MR scanner is also different, so the present results are a truly independent confirmation of the previous findings. In the present study we also studied the cortical mantle with a topographically more accurate tool, estimated the magnitude of tissue loss, and supported the structural with neuropsychological findings.

This study has strengths as well as limitations. First, to ensure that the two patient groups were comparable, EOAD and LOAD subjects were individually matched for global disease severity based on the Clinical Dementia Rating. The quality of the matching is witnessed by disease duration being very similar in the two groups (around 3 years). Second, to exclude the effect of physiological ageing that would have resulted from directly comparing EOAD and LOAD patients or from comparing both groups to a unique control group, two separate age-specific control groups were selected matching the two patient groups by age (as well as gender). Limitations include the impossibility to carry out separate analyses by *APOE* genotype due to small resulting groups, and the restricted range of neuropsychological tests that has prevented more accurate probing into specific cognitive domains, and the use of a 1.0 T scanner. However, despite our use of a marginally lower field strength (1.0 T) than is typical in clinical research (1.5 T), the scans had sufficient grey to white matter contrast and signal to noise to differentiate grey and white matter, and patients from controls. Other things being equal, 1.0 T scans may offer slightly lower contrast to noise for tissue differentiation but also suffer less from artefacts that are often pronounced at higher fields (intensity gradients in the grey and white matter due to radiofrequency field inhomogeneity, and signal fall-off due to susceptibility gradients near the sinuses).

Supplementary material

See supplementary material available at *Brain* Online.

Acknowledgements

Algorithm development for this study was supported in part by research grants from the National Center for Research Resources (P41 RR13642), the National Institute of Mental Health (RO1 MH60374), the NIH Roadmap Initiative (P20 RR020750), the National Library of Medicine (R01 LM05639) and by grants R21 EB01651, R21 RR019771 and AG016570 (to P.T.). We are indebted to Giuliano Binetti, Laboratory of Neurobiology, IRCCS Centro San Giovanni di Dio, Brescia, for providing APOE data, and to Sun Xin Yu, Institute of Mental Health, Peking University, Beijing, for help in the brain extraction for cortical pattern matching. Roberta Rossi scored white matter changes, Elisa Canu made the tracings for total

intracranial volume measurements, Samantha Galluzzi collected clinical information from patients, and Monica Ettori administered the neuropsychological tests. Marina Boccardi kindly provided useful suggestions on limbic system physiology.

References

Amodio P, Wenin H, Del Piccolo F, Mapelli D, Montagnese S, Pellegrini A, et al. Variability of trail making test, symbol digit test and line trait test in normal people. A normative study taking into account age-dependent decline and sociobiological variables. Aging Clin Exp Res 2002; 14: 117–31.

Bird TD, Stranahan S, Sumi SM, Raskind M. Alzheimer's disease: choline acetyltransferase activity in brain tissue from clinical and pathological subgroups. Ann Neurol 1983; 14: 284–93.

Boccardi M, Sabattoli F, Laakso MP, Testa C, Rossi R, Beltramello A, et al. Frontotemporal dementia as a neural system disease. Neurobiol Aging 2005; 26: 37–44.

Boekhoorn K, Joels M, Lucassen PJ. Increased proliferation reflects glial and vascular-associated changes, but not neurogenesis in the presenile Alzheimer hippocampus. Neurobiol Dis 2006; 24: 1–14.

Braak H, Braak E, Bohl J, Bratzke H. Evolution of Alzheimer's disease related cortical lesions. J Neural Transm Suppl 1998; 54: 97–106.

Caffarra P, Vezzadini G, Dieci F, Zonato F, Venneri A. Rey-Osterrieth complex figure: normative values in an Italian population sample. Neurol Sci 2002; 22: 443–7.

Carlesimo GA, Caltagirone C, Gainotti G. The Mental Deterioration Battery: normative data, diagnostic reliability and qualitative analyses of cognitive impairment. The Group for the Standardization of the Mental Deterioration. Battery. Eur Neurol 1996; 36: 378–84.

Chan D, Janssen JC, Whitwell JL, Watt HC, Jenkins R, Frost C, et al. Change in rates of cerebral atrophy over time in early-onset Alzheimer's disease: longitudinal MRI study. Lancet 2003; 362: 1121–2.

Chui HC, Teng EL, Henderson VW, Moy AC. Clinical subtypes of dementia of the Alzheimer type. Neurology 1985; 35: 1544–50.

Collins DL, Neelin P, Peters TM, Evans AC. Automatic 3D intersubject registration of MR volumetric data in standardized Talairach space. J Comput Assist Tomogr 1994; 18: 192–205.

De Renzi E, Vignolo LA. The token test: a sensitive test to detect receptive disturbances in aphasia. Brain 1962; 85: 665–78.

de Silva R, Lashley T, Strand C, Shiarli AM, Shi J, Tian J, et al. An immunohistochemical study of cases of sporadic and inherited frontotemporal lobar degeneration using 3R- and 4R-specific tau monoclonal antibodies. Acta Neuropathol (Berl) 2006; 111: 329–40.

DeCarli C, Murphy DG, Gillette JA, Haxby JV, Teichberg D, Schapiro MB, et al. Lack of age-related differences in temporal lobe volume of very healthy adults. AJNR Am J Neuroradiol 1994; 15: 689–96.

Devinsky O, Morrell MJ, Vogt BA. Contributions of anterior cingulate cortex to behaviour. Brain 1995; 118: 279–306.

Folstein MF, Folstein SE, McHugh PR. "Mini-mental State". A practical method for grading the cognitive state of patients for the clinician. J Psychiatr Res 1975; 12: 189–98.

Fox NC, Crum WR, Scahill RI, Stevens JM, Janssen JC, Rossor MN. Imaging of onset and progression of Alzheimer's disease with voxel-compression mapping of serial magnetic resonance images. Lancet 2001; 358: 201–5.

Frisoni GB, Beltramello A, Weiss C, Geroldi C, Bianchetti A, Trabucchi M. Linear measures of atrophy in mild Alzheimer disease. AJNR Am J Neuroradiol 1996; 17: 913–23.

Frisoni GB, Testa C, Sabattoli F, Beltramello A, Soininen H, Laakso MP. Structural correlates of early and late onset Alzheimer's disease: voxel based morphometric study. J Neurol Neurosurg Psychiatry 2005; 76: 112–4.

Fukutani Y, Cairns NJ, Rossor MN, Lantos PL. Cerebellar pathology in sporadic and familial Alzheimer's disease including APP 717 (Val->Ile) mutation cases: a morphometric investigation. J Neurol Sci 1997; 149: 177–84.

Gomez-Isla T, Growdon WB, McNamara MJ, Nochlin D, Bird TD, Arango JC, et al. The impact of different presenilin 1 and presenilin 2 mutations on amyloid deposition, neurofibrillary changes and neuronal loss in the familial Alzheimer's disease brain: evidence for other phenotype-modifying factors. Brain 1999; 122: 1709–19.

Gosche KM, Mortimer JA, Smith CD, Markesbery WR, Snowdon DA. Hippocampal volume as an index of Alzheimer neuropathology: findings from the Nun Study. Neurology 2002; 58: 1476–82.

Grady CL, Haxby JV, Horwitz B, Berg G, Rapoport SI. Neuropsychological and cerebral metabolic function in early vs late onset dementia of the Alzheimer type. Neuropsychologia 1987; 25: 807–16.

Haltia M, Viitanen M, Sulkava R, Ala-Hurula V, Poyhonen M, Goldfarb L, et al. Chromosome 14-encoded Alzheimer's disease: genetic and clinicopathological description. Ann Neurol 1994; 36: 362–7.

Hirao K, Ohnishi T, Matsuda H, Nemoto K, Hirata Y, Yamashita F, et al. Functional interactions between entorhinal cortex and posterior cingulate cortex at the very early stage of Alzheimer's disease using brain perfusion single-photon emission computed tomography. Nucl Med Commun 2006; 27: 151–6.

Hixson JE, Vernier DT. Restriction isotyping of human apolipoprotein E by gene amplification and cleavage with HhaI. J Lipid Res 1990; 31: 545–8.

Ho GJ, Hansen LA, Alford MF, Foster K, Salmon DP, Galasko D, et al. Age at onset is associated with disease severity in Lewy body variant and Alzheimer's disease. Neuroreport 2002; 13: 1825–8.

Hughes CP, Berg L, Danziger WL, Coben LA, Martin RL. A new clinical scale for the staging of dementia. Br J Psychiatry 1982; 140: 566–72.

Jacobs D, Sano M, Marder K, Bell K, Bylsma F, Lafleche G, et al. Age at onset of Alzheimer's disease: relation to pattern of cognitive dysfunction and rate of decline. Neurology 1994; 44: 1215–20.

Janssen JC, Beck JA, Campbell TA, Dickinson A, Fox NC, Harvey RJ, et al. Early onset familial Alzheimer's disease: Mutation frequency in 31 families. Neurology 2003; 60: 235–9.

Jin K, Peel AL, Mao XO, Xie L, Cottrell BA, Henshall DC, et al. Increased hippocampal neurogenesis in Alzheimer's disease. Proc Natl Acad Sci USA 2004; 101: 343–7.

Kemp PM, Holmes C, Hoffmann SM, Bolt L, Holmes R, Rowden J, et al. Alzheimer's disease: differences in technetium-99 m HMPAO SPECT scan findings between early onset and late onset dementia. J Neurol Neurosurg Psychiatry 2003; 74: 715–9.

Klünemann HH, Fronhöfer W, Wurster H, Fischer W, Ibach B, Klein HE. Alzheimer's second patient: Johann F. and his family. Ann Neurol 2002; 52: 520–3.

Kono K, Kuzuya F, Yamamoto T, Endo H. Comparative study of cerebral ventricular dilation and cognitive function in patients with Alzheimer's disease of early versus late onset. J Geriatr Psychiatry Neurol 1994; 7: 39–45.

Kril JJ, Halliday GM. Clinicopathological staging of frontotemporal dementia severity: correlation with regional atrophy. Dement Geriatr Cogn Disord 2004; 17: 311–5.

Lantos PL, Luthert PJ, Hanger D, Anderton BH, Mullan M, Rossor M. Familial Alzheimer's disease with the amyloid precursor protein position 717 mutation and sporadic Alzheimer's disease have the same cytoskeletal pathology. Neurosci Lett 1992; 137: 221–4.

Larner AJ, du Plessis DG. Early-onset Alzheimer's disease with presenilin-1 M139V mutation: clinical, neuropsychological and neuropathological study. Eur J Neurol 2003; 10: 319–23.

Lemere CA, Lopera F, Kosik KS, Lendon CL, Ossa J, Saido TC, et al. The E280A presenilin 1 Alzheimer mutation produces increased A beta 42 deposition and severe cerebellar pathology. Nat Med 1996; 2: 1146–50.

MacDonald D, Avis D, Evans A. Multiple surface identification and matching in magnetic resonance imaging. Proc SPIE 1994; 2359: 160–9.

Mann DM, Iwatsubo T, Cairns NJ, Lantos PL, Nochlin D, Sumi SM, et al. Amyloid beta protein (Abeta) deposition in chromosome 14-linked

Alzheimer's disease: predominance of Abeta42(43). Ann Neurol 1996; 40: 149–56.

Maurer K, Volk S, Gerbaldo H. Auguste D and Alzheimer's disease. Lancet 1997; 349: 1546–9.

McKhann G, Drachman D, Folstein M, Katzman R, Price D, Stadlan EM, et al. Clinical diagnosis of Alzheimer's disease: report of the NINCDS-ADRDA Work Group under the auspices of Department of Health and Human Services Task Force on Alzheimer's Disease. Neurology 1984; 34: 939–44.

Mori E, Hirono N, Yamashita H, Imamura T, Ikejiri Y, Ikeda M, et al. Premorbid brain size as a determinant of reserve capacity against intellectual decline in Alzheimer's disease. Am J Psychiatry 1997; 154: 18–24.

Mosconi L, Pupi A, De Cristofaro MT, Fayyaz M, Sorbi S, Herholz K. Functional interactions of the entorhinal cortex: an 18F-FDG PET study on normal aging and Alzheimer's disease. J Nucl Med 2004; 45: 382–92.

Novelli G, Papagno C, Capitani E, Laiacona M, Vallar G, Cappa SF. Tre test clinici di ricerca e produzione lessicale. Taratura su soggetti normali. Arch Psicol Neurol Psichiatr 1986; 47: 477–506.

Pruessner JC, Li LM, Serles W, Pruessner M, Collins DL, Kabani N, et al. Volumetry of hippocampus and amygdala with high-resolution MRI and three-dimensional analysis software: minimizing the discrepancies between laboratories. Cereb Cortex 2000; 10: 433–42.

Reitan RM. Validity of the trailmaking test as an indication of organic brain damage. Percept Mot Skills 1958; 8: 271–6.

Riello R, Sabattoli F, Beltramello A, Bonetti M, Bono G, Falini A, et al. Brain volumes in healthy adults aged 40 years and over: a voxel-based morphometry study. Aging Clin Exp Res 2005; 17: 329–36.

Rogaeva E. The solved and unsolved mysteries of the genetics of early-onset Alzheimer's disease. Neuromolecular Med 2002; 2: 1–10.

Rossor MN, Iversen LL, Reynolds GP, Mountjoy CQ, Roth M. Neurochemical characteristics of early and late onset types of Alzheimer's disease. Br Med J 1984; 288: 961–4.

Sakamoto S, Ishii K, Sasaki M, Hosaka K, Mori T, Matsui M, et al. Differences in cerebral metabolism between early and late onset types of Alzheimer's disease. J Neurol Sci 2002; 200: 27–32.

Scahill RI, Schott JM, Stevens JM, Rossor MN, Fox NC. Mapping the evolution of regional atrophy in Alzheimer's disease: unbiased analysis of fluid-registered serial MRI. Proc Natl Acad Sci USA 2002; 99: 4703–7.

Seltzer B, Sherwin I. A comparison of clinical features in early- and late-onset primary degenerative dementia. One entity or two? Arch Neurol 1983; 40: 143–6.

Shattuck DW, Sandor-Leahy SR, Schaper KA, Rottenberg DA, Leahy RM. Magnetic resonance image tissue classification using a partial volume model. Neuroimage 2001; 13: 856–76.

Sheitman BB, Lieberman JA. The natural history and pathophysiology of treatment resistant schizophrenia. J Psychiatr Res 1998; 32: 143–50.

Shiino A, Watanabe T, Maeda K, Kotani E, Akiguchi I, Matsuda M. Four subgroups of Alzheimer's disease based on patterns of atrophy using VBM and a unique pattern for early onset disease. Neuroimage 2006; 33: 17–26.

Singleton AB, Hall R, Ballard CG, Perry RH, Xuereb JH, Rubinsztein DC, et al. Pathology of early-onset Alzheimer's disease cases bearing the Thr113-114ins presenilin-1 mutation. Brain 2000; 123: 2467–74.

Smith AD. Imaging the progression of Alzheimer pathology through the brain. Proc Natl Acad Sci USA 2002; 99: 4135–7.

Sowell ER, Thompson PM, Rex D, Kornsand D, Tessner KD, Jernigan TL, et al. Mapping sulcal pattern asymmetry and local cortical surface GM distribution *in vivo*: maturation in perisylvian cortices. Cereb Cortex 2002; 12: 17–26.

Spinnler H, Tognoni G. Standardizzazione e taratura italiana di test neuropsicologici. Ital J Neurol Sci 1987; 6 Suppl 8.

Sullivan EV, Pfefferbaum A, Swan GE, Carmelli D. Heritability of hippocampal size in elderly twin men: equivalent influence from genes and environment. Hippocampus 2001; 11: 754–62.

Thompson PM, Woods RP, Mega MS, Toga AW. Mathematical/computational challenges in creating deformable and probabilistic atlases of the human brain. Hum Brain Mapp 2000; 9: 81–92.

Thompson PM, Cannon TD, Narr KL, van Erp T, Poutanen VP, Huttunen M, et al. Genetic influences on brain structure. Nat Neurosci 2001; 4: 1253–8.

Thompson PM, Hayashi KM, de Zubicaray G, Janke AL, Rose SE, Semple J, et al. Dynamics of GM loss in Alzheimer's disease. J Neurosci 2003; 23: 994–1005.

Thompson PM, Hayashi KM, Sowell ER, Gogtay N, Giedd JN, Rapoport JL, et al. Mapping cortical change in Alzheimer's disease, brain development, and schizophrenia. Neuroimage 2004; 23 Suppl 1: S2–18.

Van Leemput K, Maes F, Vandermeulen D, Suetens P. Automated model-based bias field correction of MR images of the brain. IEEE Trans Med Imaging 1999a; 18: 885–96.

Van Leemput K, Maes F, Vandermeulen D, Suetens P. Automated model-based tissue classification of MR images of the brain. IEEE Trans Med Imaging 1999b; 18: 897–908.

Vogt BA, Finch DM, Olson CR. Functional heterogeneity in cingulate cortex: the anterior executive and posterior evaluative regions. Cereb Cortex 1992; 2: 435–43.

Wahlund LO, Barkhof F, Fazekas F, Bronge L, Augustin M, Sjogren M, et al. A new rating scale for age-related white matter changes applicable to MRI and CT. Stroke 2001; 32: 1318–22.

Wang CC, Kadota M, Nishigaki R, Kazuki Y, Shirayoshi Y, Rogers MS, et al. Molecular hierarchy in neurons differentiated from mouse ES cells containing a single human chromosome 21. Biochem Biophys Res Commun 2004; 314: 335–50.